Astronomy & Astrophysics manuscript no.
(will be inserted by hand later)

arXiv:astro-ph/0207495v1 23 Jul 2002

A sample of southern Compact Steep Spectrum radio sources: The VLBI observations ⋆

A. Tzioumis[1], E. King[6,11], R. Morganti[3], D. Dallacasa[2,9], C. Tadhunter[4], C. Fanti[2,10], J. Reynolds[1], D. Jauncey[1], R. Preston[5], P. McCulloch[6], S. Tingay[1], P. Edwards[7,12], M. Costa[6], D. Jones[5], J. Lovell[6,1], R. Clay[7], D. Meier[5], D. Murphy[5], R. Gough[1], R. Ferris[1], G. White[8], P. Jones[8]

[1] ATNF – CSIRO, Epping, Australia
[2] Istituto di Radioastronomia – CNR, via Gobetti 101, I-40129 Bologna, Italy
[3] Netherlands Foundation for Research in Astronomy, Postbus 2, NL-7990 AA, Dwingeloo, The Netherlands
[4] Department of Physics, University of Sheffield, UK
[5] Jet Propulsion Laboratory, Caltech, Pasadena, CA, USA
[6] University of Tasmania, Hobart, Tasmania, Australia
[7] University of Adelaide, Adelaide, SA, Australia
[8] University of Western Sydney, Kingswood, NSW, Australia
[9] Astronomy Dept. Università di Bologna, via Ranzani 1, I-40127 Bologna, Italy
[10] Physics Dept. Università di Bologna, via Irnerio 46, I-40126 Bologna, Italy
[11] COSSA/EOC – CSIRO, Canberra, Australia
[12] ISAS, Sagamihara, Kanagawa, Japan

Received 11-03-02; accepted 26-06-02

Abstract. A small sample of 7 southern Compact Steep Spectrum (CSS) radio sources has been selected as part of the study of a larger flux-limited complete sample of radio sources. High resolution images, using the VLBI network in the southern hemisphere and the high resolution MERLIN array, are presented for all sources in the CSS sample. The overall morphology of each source consists of well-defined double lobes but with substantial diffuse and extended components present. In the majority of cases only a fraction of the total flux density is detected on the VLBI baselines, indicating the presence of larger extended radio structures. However, all sources are unresolved at arcsecond scales and are of sub-galactic size, with linear size in the range 0.1–2 kpc. The radio properties of the sources agree well with CSS sources in other samples.

Key words. Galaxies: active, Radio continuum: general

1. Introduction

Among the many open questions about powerful radio-galaxies is the early evolution of these objects. This is an important issue not only from the point of view of the detailed phenomenology of these objects but also for understanding the evolution of massive galaxies. Galaxies in their early stage of radio activity are likely to have their nuclear regions enshrouded in a cocoon or thick disk of material left over from the event(s) that trigger the activity. The radio jet expanding in this medium will interact and sweep out this rich interstellar medium (ISM). These processes have been suggested to profoundly affect even the star formation history in luminous galaxies (Silk & Rees 1998). Thus, the study of the early-phase of radio activity and its effect on the galaxy medium has broad implications.

Compact Steep Spectrum (CSS) and Gigahertz Peaked Spectrum (GPS) radio sources have now been recognised to be the likely candidates of radio sources in such an early stage of their life. These radio sources are powerful ($P_{2.7GHz} \gtrsim 10^{25.5}$ W Hz^{-1}), have a steep spectral index at high frequencies ($\alpha < -0.5$, $S \sim \nu^{\alpha}$) and sub-galactic size (<20 kpc). Indeed, the turnover often observed in their spectra (around 1 GHz for the GPSs and about 100 MHz for the CSSs) is usually interpreted as synchrotron self-absorption, with the frequency of this turnover varying with the linear scale of the source, although free-free absorption may also play a role (Bicknell et al. 1997). A review of the characteristics of CSS/GPS sources at different wavelengths is given in O'Dea (1998).

The age of CSS/GPS sources has been recently estimated using both the lobe proper motion (e.g. Owsianik

Send offprint requests to: A.Tzioumis

⋆ Based on observations with the Southern Hemisphere VLBI Network (SHEVE) and the MERLIN.

& Conway 1998) and the radiative ages (Murgia et al. 1999). The ages derived are less than a few thousand years, therefore strongly supporting the *"youth" scenario* in the interpretation of these sources. A summary of the results is given in the review by Fanti et al. (2000).

The sub-galactic size and the young age of these sources makes them an extremely interesting class of radio source. They can be used to probe further the characteristics of the ISM in the early phase of radio source evolution and the effects of the radio plasma expanding in this medium. This has been done in a restricted number of objects both using the atomic hydrogen (e.g. Conway 1996, Pilström 2001, Morganti et al. 2001, Peck & Taylor 2001) and the ionised gas (e.g. Gelderman & Whittle 1994, Morganti et al. 1997, Axon et al. 2000, O'Dea et al. 2002).

An other important aspect in the study of these objects is the comparison of their characteristics with those of the extended radio galaxies. This has been done quite extensively in the radio to investigate the evolutionary scenario. At wavelengths different from radio the available data are still limited. ISO observations (Fanti et al. 2000) and optical and near IR data (de Vries et al. 1998) showed no significant difference between CSS/GPS sources and extended radio galaxies with similar radio power, failing therefore to detect any extra component capable to "frustrate" the CSS/GPS sources.

To extend the comparison between the optical properties of CSS/GPS and extended radio sources, a group of CSS/GPS sources was selected from a complete subsample of the *2 Jy sample of radio sources* (see Sect. 2 for details). Optical spectra were obtained for both the compact as well as for the extended sources in this sample (see Tadhunter et al. 1993) and the spectral characteristics could therefore be compared for objects in a similar range of redshift and radio power. A first-order similarity was found between the spectra of CSS/GPS sources and the extended source of similar radio power although the former may be of slightly lower ionisation, possible evidence for the compression effect of shocks due to jet/cloud interaction (Morganti et al. 1997). For the 2 Jy CSS/GPS source sample however, there is a lack of high resolution radio images capable of providing information on their morphology. Most of the well studied CSS/GPS galaxies tend to have symmetric, double-lobed radio structures (e.g. Dallacasa et al. 1995, O'Dea 1998), reminiscent of scale-down versions of extended, edge-brightened Fanaroff-Riley II sources. Collecting this information for the CSS/GPS sources in the 2 Jy sample is particularly important also for the interpretation of their optical data. The presence of more complex radio morphology in these sources (or in some of them) would be an indication of a particularly strong interaction between the radio plasma and the ISM, more than usually found in this type of radio source.

In order to fill this gap, in this paper we present and discuss new high resolution (VLBI and MERLIN) data for this group of seven 2 Jy CSS/GPS sources. These radio images permit a proper morphological classification of the sub-kpc radio emission in these objects.

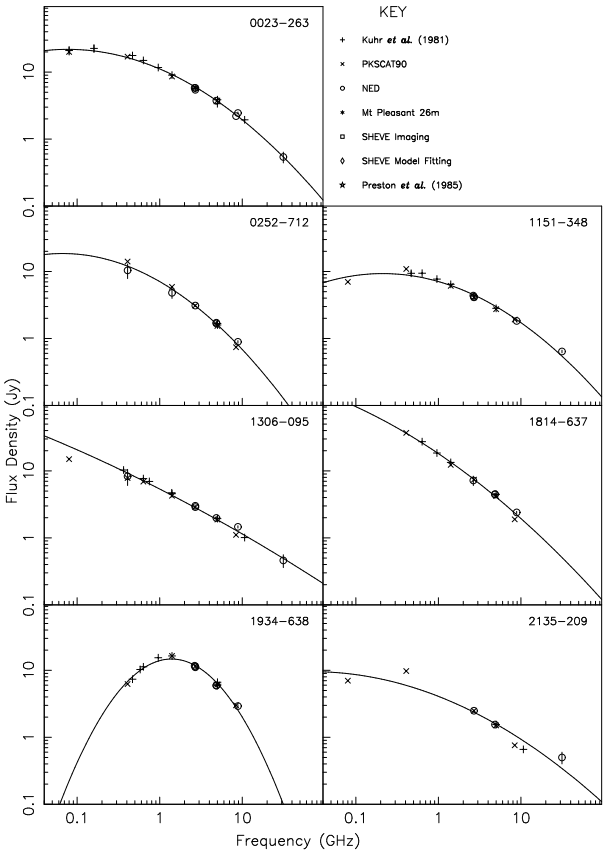

Fig. 1. Radio spectral index plots for all sources.

Name	ID	m_V	z	scale pc/mas	log $P_{2.7\ GHz}$ W Hz^{-1}	$\alpha_{2.7}^{8.4}$
$0023-263$	G	19.5	0.322	2.9	26.91	-0.8
$0252-712$	G	20.9	0.566	3.7	27.28	-1.25
$1151-348$	Q	17.8	0.258	2.5	26.56	-0.7
$1306-095$	G	20.5	0.464	3.5	26.94	-0.85
$1814-637$	G	18.0	0.063	0.8	25.54	-1.2
$1934-638^*$	G	18.4	0.183	2.0	26.68	-1.15
$2135-209$	G	19.4	0.635	3.9	27.20	-1.05

* Gigahertz-Peaked Spectrum source (GPS)

Table 1. CSS sources in the sample with a summary of their characteristics.

2. The Sample

The group of CSS/GPS sources considered here has been selected from the complete sub-sample of the Wall & Peacock 1985 (WP85) 2 Jy sample described in Tadhunter et al. 1993. This sub-sample is formed by 88 radio sources (radio galaxies and quasars) having $S_{2.7GHz}$ >2.0 Jy, $\delta <$ 10° and z <0.7. The sample has been studied extensively at various wavelengths: optical (Tadhunter et al. 1993, 1998), radio (Morganti et al. 1993, 1997, 1999, Venturi

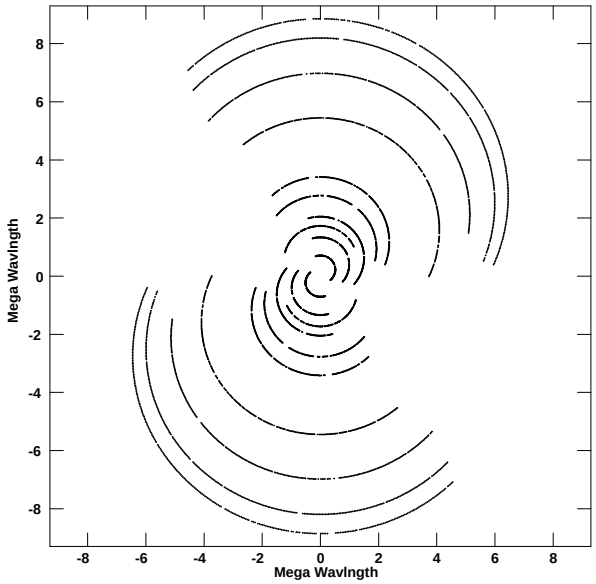

Fig. 2. Typical uv coverage of the SHEVE array, from the 0252-712 at 2.3 GHz. (No detections to Perth or Hartebeesthoek).

et al. 2000) and X-ray (Siebert et al. 1996, Padovani et al. 1999, Trussoni et al. 1999).

According to the definition in Fanti et al. 1995, a source is classified as CSS when at high frequency $\alpha < -0.5$ ($S \sim \nu^{\alpha}$) and the linear dimensions are $\leq$ 15kpc[1]. To make the selection consistent with previous works of Fanti et al. 1990 and Spencer et al. 1991, only objects with $P_{2.7\ \mathrm{GHz}} > 10^{25.5}$ W Hz^{-1} were selected. With these criteria we find 7 CSS (6 galaxies and 1 quasar) in our complete sample *i.e.* 8% of the total number of sources or 12.5% of the $P_{2.7\ \mathrm{GHz}} > 10^{25.5}$ W Hz^{-1} sub-sample.

The seven CSS sources in our sample are listed in Table 1 together with some additional information. Their radio power is consistent with the typical radio power for this class of objects. Optical identifications and redshifts (WP85; di Serego Alighieri et al. 1994) are available for every source in this sample. All sources with declination north of -40° are unresolved in VLA images ($\theta < 3''$) and the remaining are part of the ATCA calibration list ($\theta < 1''$). Radio spectra from the present radio observations and from data in the literature (King 1994) are presented in Fig. 1. The two-point spectral index $\alpha_{2.7}^{8.4}$ listed in Table 1 clearly demonstrates the steep spectrum nature of these objects.

3. Observations, data reduction and analysis

The VLBI observations of all sources were made with the SHEVE network (Preston et al. 1993; Jauncey et al. 1994) between April 1991 and February 1993, using the MK2 recording system (Clark, 1973). The characteristics of the antennas and receivers in the SHEVE network are listed in Table 2. The details of each observation are given in Table 3.

Fig. 4. PKS 0023-263 at 4996 MHz from the MERLIN array. The peak level is 1.41 Jy/beam and contours are shown at -6,-3,-1.5,-0.75,0.75,1.5,3,6,12,24,48,96 % of the peak.

All sources were observed at 2.3 GHz, but for $2135-209$ only a single baseline (Tidbinbilla-Hobart) was obtained in a 12 hour observation. The sources $0023-263$, $1151-348$ and $1934-638$ were also observed at 8.4 GHz and $1934-638$ at 4.9 GHz as well. The GPS source $1934-638$ was observed as part of another program and the details of the observations and results are presented elsewhere (King 1994; Tzioumis et al. 1996) while some discussion of the source properties is presented here.

The tapes recorded at each station were processed at the Caltech–JPL Block2 correlator in Pasadena and the NRAO AIPS package was used for global fringe fitting. The amplitude calibration and editing of the visibilities were subsequently performed using the Caltech VLBI package. Self-calibration and imaging of the data were performed using DIFMAP (Shepherd et al. 1994) and the AIPS packages. The single-baseline data for $2135-209$ was used to obtain a simple model of the source using the program MODELFIT from the Caltech VLBI package.

On the very long baselines from the antennas at eastern Australia (ATNF, DSN, Hobart) to Perth (3000 km) and Hartebeesthoek (9500 km), only $1934-638$ and VLBI calibrator sources were detected, i.e. all other sources are completely resolved out at these spacings and sensitivities. This implies that there are no very compact components ($\theta << 3$mas) with flux density larger than about 40 mJy, the detection limit from the intercontinental baselines.

A "typical" uv-coverage from the SHEVE array is presented in Fig. 2, for the source 0252-712 at 2.3 GHz. Note that all sources except 1934-638, were not detected on the long baselines to Perth or Hartebeesthoek and uv-tracks are not shown.

The limited number of antennas in the network and the lack of short baselines limit the dynamic range achievable from these observations. In particular, for many of the sources the total flux density in the VLBI images is significantly lower than that measured with lower resolution observations. This implies that low surface brightness ex-

[1] $H_{\circ} = 100$ km s^{-1} Mpc^{-1}, $q_{\circ}$=0.5

Key	Antenna	Size (m)	SEFD (Jy) 2.3 GHz	8.4 GHz
P	Parkes(ATNF)	64	90	90
M	Mopra (ATNF)*	22	400	400
C	Narrabri-CA (ATNF)	22	400	400
3	Tidbinbilla (DSS43)	70	15	20
5	Tidbinbilla (DSS45)	34	165	130
2	Tidbinbilla (DSS42)	34	100	130
H	Hobart (Univ.Tasmania)	26	750	650
G	Perth (ESA)	15	3300	–
E	Harteebeesthoek	26	400	950

* The Mopra antenna became operational in late 1991.

Table 2. Antennas participating in the VLBI observations. Note that the three Tidbinbilla antennas are at essentially the same location and only one antenna is used at any one time, depending on availability. The SEFD (system equivalent flux density) is given by the ratio between system temperature (°K) and gain °K/Jy.

Source	Epoch	Freq. GHz	Duration (hours)	Stations	B_{max}* $M\lambda$	Beam mas	°	Dynamic Range	σ mJy/beam	Figure Ref.
0023−263	1991.34	2.29	11.5	32PHC	10.5	31×14	-82	60:1	4.5	3
	1991.90	8.42	11	32PHCM	29.9	13×5	-77	40:1	1.7	3
	1992.05	4.99	6	MERLIN	3.6	168×86	-2	130:1	3.5	4
0252−712	1993.14	2.29	10.25	2PHCMGE	8.9	32×19	-73	65:1	8	5
1151−348	1991.34	2.29	11.75	35PHC	10.7	29×13	89	70:1	4.5	6
	1992.24	8.42	11	35PHCM	30.3	11×5	81	35:1	3.6	6
1306−095	1993.14	2.29	10.5	32PHCGE	10.7	48×15	-73	20:1	5.7	7
1814−637	1993.14	2.29	12	32PHCMGE	9.5	32×17	-86	50:1	5.8	8
1934−638	*2.29, 4.85 & 8.42 GHz images in King, 1994 & Tzioumis et al. 1996*									10
2135−209	1991.55	2.29	12	3H	3.6	*Modelfit only*				
	1992.91	4.99	6.25	MERLIN	3.6	163×34	10	130:1	2.3	9

* Maximum baseline with significant dectection of each source. No detections to Perth (G) or Hartebeesthoek (E).

Table 3. Observations and images presented in this paper. The dynamic range indicates the ratio of the peak brightness in the image to the peak in the residual map. The σ_{rms} entry refers to the residual rms noise in regions devoid of any source emission. Entries in the last column refer to the figure in which each image appears.

tended structures with angular sizes between 0.1 and 1 arcsec are often present but invisible by the VLBI interferometers, as discussed in the next section on each source.

For 0023−263 and 2135−209 we also present MERLIN observations at 5.0 GHz, which provide information on more extended structures, not detected by the VLBI observations.

The new images of the six sources observed in this program are presented in Figs. 3 through 9. Restoring beams together with the noise measure on the image plane are given in Table 3.

The overall size of most sources in this sample was not previously well determined at radio wavelengths. The largest angular/linear size for each source was estimated from the images, adopting a "low resolution" approach (cf. Dallacasa et al. 1995). Most of the sources show distinct and well separated "lobes", and extended structure can be seen in most of them. Their sizes and flux densities were estimated from the images and are summarised in Table 5. The component angular dimensions were generally estimated directly from the images (except were otherwise stated) by considering the lowest reliable contour; they are given as full-width axis sizes. This approach was adopted because almost all components show extended structures and it is then difficult to fit single Gaussian components. The measurements provided values well in excess of the beam size, and they were not deconvolve given they would not change significantly; therefore, all sizes in Table 5 should be treated as upper limits.

The separation between the strongest component in each of the lobes was also measured from the images. This separation is a very sensitive parameter since it is well determined by the "beating" in the visibilities and can be used to search for any source expansion in time, even with sparse uv coverage. The results are presented in Table 4.

For the two sources observed at 2.3 and 8.4 GHz, a two-point spectral index for each lobe has also been determined.

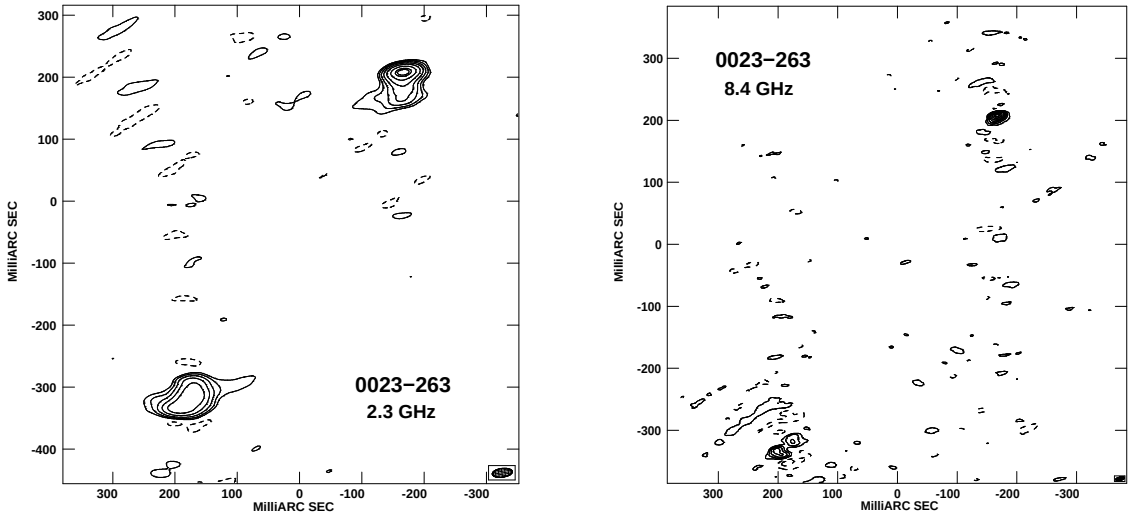

Fig. 3. (*Left*) PKS 0023-263 at 2291 MHz from the SHEVE array. The peak level is 1.07 Jy/beam and contours are shown at -2,-1,1,2,4,8,16,35,65,80 % of the peak. (*Right)* PKS 0023-263 at 8419 MHz from the SHEVE array. The peak level is 0.41 mJy/beam and contours are shown at -2,-1,1,2,4,8,16,35,65,80 % of the peak.

Source	Comp.	ν	θ_1	θ_2	Lsize1	Lsize2	S_{peak}	$S_{tot.}$	$\alpha_{2.3}^{8.4}$
		GHz	mas	mas	pc	pc	Jy/beam	Jy	
$0023-263$	NW	2.3	80	75	230	220	1.07	1.6	-0.7
		8.4	40	23	110	65	0.41	0.65	
	SE	2.3	100	90	290	260	0.33	1.3	-1.3
		8.4	60	30	175	85	0.047	0.25	
$0252-712$	North	2.3	110	90	400	330	1.14	2.1	
	South		120	90	440	330	0.47	1.4	
$1151-348$	NE	2.3	85	45	210	110	1.57	2.1	-0.6
		8.4	40	30	100	75	0.437	0.94	
	SW	2.3	85	45	210	110	0.78	1.24	-1.0
		8.4	35	20	90	50	0.12	0.36	
$1306-095$	SE	2.3	110	70	380	240	0.304	0.76	
	NW		80	50	275	170	0.107	0.15	
$1814-637$	North	2.3	90	80	70	65	1.58	2.8	
	South		130	70	100	55	0.380	1.8	
$1934-638^a$									
$2135-209^b$	NE	5.0	25	9	100	350	1.02	1.1	
	SW		90	40	350	155	0.2	0.36	

[a] Components and spectra for $1934-638$ are given in Tzioumis et al. 1996.

[b] Component sizes from fitting Gaussians (FWHM) since the beam is comparable to the source size and components cannot be estimated graphically.

Table 5. Size and flux density of the components in the images. Component angular sizes are estimated from the images (full width), except were otherwise noted.

4. Comments on individual sources

In the following, a description of the morphology of each source is given:

0023-263 This radio source has been identified with a galaxy of $m_v = 19.5$ by WP85 at a redshift of 0.322 (Tadhunter et al. 1993; di Serego Alighieri et al. 1994). The VLBI images at 2.3 and 8.4 GHz are shown in Fig. 3.

At both VLBI frequencies this radio galaxy shows a basic double structure with a separation of $\sim$ 650 mas

Name	θ_{max}	Lin. size	Component separation θ	l	Orientation
	mas	pc	mas	pc	°
$0023-263$	680	1970	654	1900	-34
$0252-712$	240	900	145	540	7
$1151-348$	170	425	91	228	72
$1306-095$	460	1600	373	1290	-41
$1814-637$	410	328	239	191	-20
$1934-638^*$	70	140	42	84	89
$2135-209$	∼250	∼1000	167	650	52

* Tzioumis et al. 1996

Table 4. Overall angular and linear sizes of the sample sources and separation of strongest components in the two lobes.

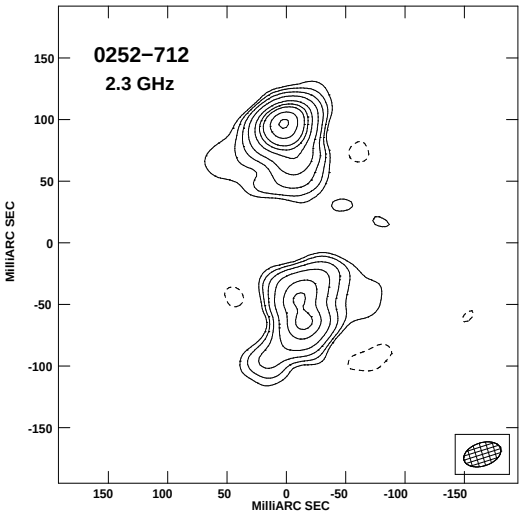

Fig. 5. PKS 0252-712 at 2291 MHz from the SHEVE array. The peak level is 1.14 Jy/beam and contours are shown at -1.5,1.5,3,6,12,24,36,48,72,96 % of the peak.

(∼1.9kpc) in p.a. −34° between the peak brightness of each lobe. Both radio emitting regions are complex and extended structures are evident. In particular, the south-eastern component is resolved into two sub-components embedded into more diffuse emission. Thus, it is not possible to fit simple Gaussian components, and sizes for each lobe are estimated from the images. Both lobes are less than ∼100 mas (∼ 0.3kpc) in extent and the south-eastern one has an overall spectral index (α=–1.3) steeper than the north-western component (α=–0.7), possibly also because it is more resolved.

The flux density detected in the VLBI images accounts for only about 40% of the total source flux density at each frequency. This indicates that there is undetected extended scale structures in the range 0.1 to 1 arcseconds. The same fraction of flux density is undetected at both frequencies, suggesting that the underlying diffuse structure has similar spectral index (∼ −0.9) to the components visible in the images. No flat spectrum component indicative of a core is detected between the lobes at the detection limits (5σ) of ∼20 mJy/beam at 2.3 GHz and ∼10 mJy/beam at 8.4 GHz. We decided to use 5 σ as detection limit for the cores (in this and in the following sources), given that, the complexity of the radio emission in relation to the limited uv-sampling, increases the incidence of clean artifacts at lower levels.

The MERLIN image at 5 GHz (Fig. 4) with much lower resolution shows the basic double-lobe structure of the source and the extended emission surrounding the lobes. About 90% of he total flux density is detected (3.4 Jy out of 3.8 Jy) indicating little extended emission at arcsecond scales.

0252-712 This object has been identified with a galaxy of m_V=20.9 and redshift z = 0.566 (di Serego Alighieri et al. 1994). The VLBI image at 2.3 GHz (Fig. 5) shows a North-South double structure quite symmetric; the peak regions are separated by ∼145 mas (∼0.54 kpc). Both components appear to be resolved and account for more than 95% of the whole flux density of 3.7 Jy at this frequency. No "core" component is detected between the lobes (5σ=40 mJy) and no spectral information is available on the detected components.

1151-348 This object has been identified as a quasar with m_v = 17.8 from WP85 and z = 0.258 (Jauncey et al. 1978). Both 2.3 and 8.4 GHz images are available (Fig 6), showing two components with separation of 91 mas (∼ 0.23 kpc) and p.a.= 72° and possibly some extended emission between them. The peak separation and orientation are identical (to within 0.5 mas) at both frequencies, unambiguously registering the two components.

Both lobes are less than ∼85 mas (∼ 0.2kpc) in extent and the south-western one has an overall spectral index (α=–1.0) steeper than the north-eastern component (α=–0.6). About 70% of the total flux density is detected in the VLBI components and this fraction is the same at both frequencies. Thus the underlying undetected flux density has a spectral index (∼–0.7) similar to the two aforementioned components, possibly indicating that this emission is simply resolved, diffuse extension of these lobes.

No flat spectrum component, possibly indicative of a core, is detected between the lobes, at the detection limit (5σ) of ∼20 mJy/beam.

1306-095 It is identified with a galaxy of magnitude m_V=20.5 and redshift z=0.464 (di Serego Alighieri et al. 1994).

This source is at low absolute declination and the uv coverage is rather poor, which implies high sidelobe levels (∼50%) and a low dynamic range image. The radio emission is dominated by two distinct components separated

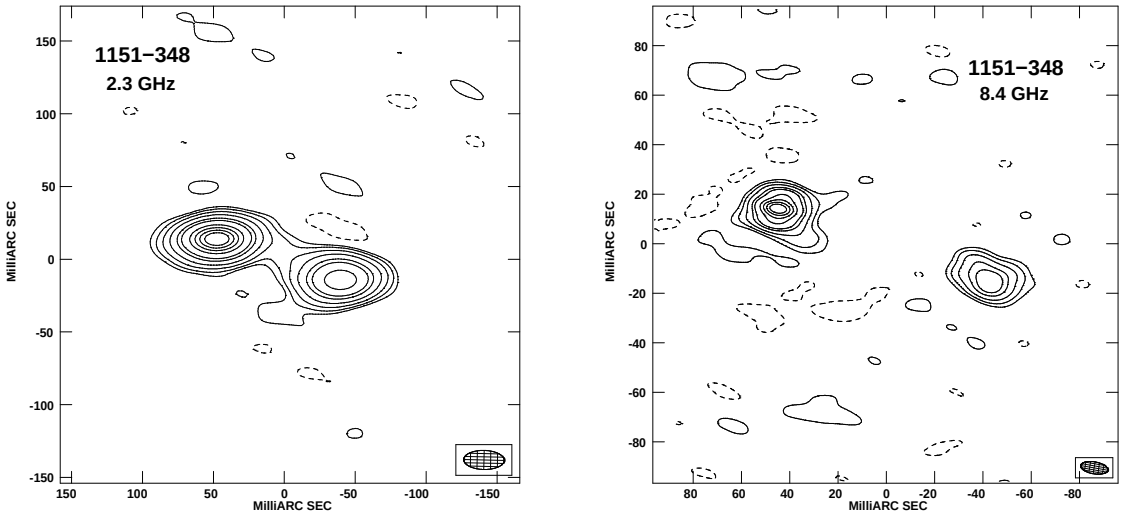

Fig. 6. (*Left*) PKS 1151-348 at 2291 MHz from the SHEVE array. The peak level is 1.57 Jy/beam and contours are shown at -0.75,0.75,1.5,3,6,12,18,35,50,65,80 % of the peak. (*Right*) PKS 1151-348 at 8421 MHz from the SHEVE array. The peak level is 0.44 Jy/beam and contours are shown at -1.5,1.5,3,6,12,18,35,50,65,80 % of the peak.

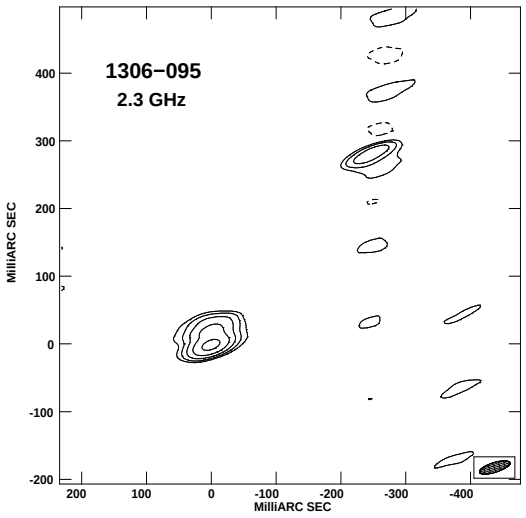

Fig. 7. PKS 1306-095 at 2291 MHz from the SHEVE array. The peak level is 0.30 Jy/beam and contours are shown at -5,5,10,20,40,80 % of the peak.

by about 373 mas (∼1.3 kpc) in p.a. ∼ −40° (Fig. 7). The southern component is much stronger, accounting for more than 80% of the detected flux density. Only about 30% of the total flux density is detected by the VLBI components, indicating the presence of much diffuse emission completely resolved out by the VLBI baselines. It is likely that in Fig 7 only the hot-spots of two mini-lobes are visible.

1814-637 It is identified with a galaxy of $m_V = 18.0$ with $z = 0.063$ by WP85. The VLBI image at 2.3 GHZ shows the most complex structure of all sources in this sample (Fig. 8). The source still shows a basic double-lobed structure aligned almost North-South. However, the southern region is dominated by two components with similar brightness and much extended emission. The northern region shows a prominent bright component and extended emission, with possible North-South symmetrical extensions, but the overall extent of this component is still less than ∼90 mas (∼70 pc).

Just over 50% of the total flux density of the source is detected, indicating the presence of further, much more diffuse extended component. The overall source size is still less than about 0.5 arcsecond and no arcsecond-scale components are detected with ATCA observations.

There is also a weak component between the two major lobes at the 5% level, which corresponds to a 15σ detection. This can be just a peak in the underlying diffuse component or could indicate the presence of a core between the two lobes. VLBI observations at another frequency are needed to determine the spectrum of this component and decide whether it is the core.

1934-63 This compact radio source has been identified as a galaxy with $m_V = 18.4$ by Kellerman (1966) and has redshift $z = 0.183$ (Penston & Fosbury 1978). A VLBI image at 2.3 GHz from observations carried out in 1982 has been presented in Tzioumis et al. (1989) and preliminary images at 2.3, 4.8 and 8.4 GHz have also been presented elsewhere (King 1994; Tzioumis et al. 1996). The knowledge about the pc-scale structure of this source is summarised in Fig. 10. The source appears as a very compact

double, with component separation of 42 mas ($\sim$ 0.084 kpc) in p.a. 89°, and this separation has not changed for over 15 years. As reported in Tzioumis et al. (1996), this yield to an upper limit to the expansion velocity of $0.2c$. The total flux density of the source is detected by the VLBI components and there is no definite detection of a flat-spectrum core component at a level of a few % of the peak at any frequency.

2135-209 This source is a galaxy with $m_v = 19.4$ and $z = 0.635$ (WP85 and di Serego Alighieri et al. 1994) .

No VLBI image exists for this source and here we present a MERLIN 5 GHz image (Fig. 9). The source shows a double lobed very asymmetric structure; the resolution of MERLIN at this southern declination is poor (163×34 mas in the case of 2135-209) to allow further consideration on the morphology. Because of the limited resolution compared to the source extension, the component parameters were derived by means of Gaussian fitting. The North–East dominant component is marginally resolved and accounts for more than 80% of the detected flux density. The total flux density of about 1.5 Jy was detected in the MERLIN image, indicating no extra extended components exist.

From one-baseline VLBI observations at 2.3 GHz it is possible to fit models to the double structure. The strong north-east component is unresolved while the south-west component is extended. The separation between the peaks in the two lobes is well determined at 167 mas ($\sim$0.65 kpc), at a position angle of 52°, close to the position angle and separation determined from the MERLIN image. About 85% of the total flux density is detected on this VLBI baseline.

5. Discussion

The main aim of these high resolution observations was the morphological classification of a group of CSS sources found in a larger, flux-limited sample mainly consisting of extended radio sources. Like the majority of CSS sources studied in previous works, the objects observed here show mainly a double-lobed structure, often asymmetric. The structures revealed by these observations are generally resolved and they may well represent the lobes of small-sized powerful radio sources. In fact, for the two sources observed at both 8.4 and 2.3 GHz, only steep spectrum components have been detected. The present observations do not reveal any definite core candidates, but in one case ($1814-637$) there is a weak third component between the lobes which could be suggested as a possible core. Weak tails are found pointing towards the source centre in a few cases, further suggesting that we are seeing two-sided emission from lobes and possibly hot-spots.

Generally, these images do not show many highly distorted or complex structures, which could be ascribed either to the interaction between the radio emitting plasma and the ambient medium or to projection effects. Even in the object which shows the most complex structure ($1814-637$), the basic double-lobed morphology is still clearly evident. Source linear sizes are in the range 0.08–2.9 kpc, and hence all sources in this sample can be classified as compact symmetric (CSO) or medium-sized symmetric (MSO) objects if we assume that an undetected core sits between the lobes revealed by the present observations.

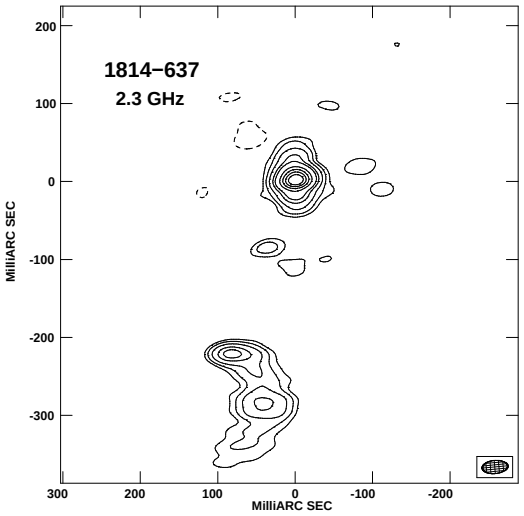

Fig. 8. PKS 1814-637 at 2291 MHz from the SHEVE array. The peak level is 1.7 Jy/beam and contours are shown at -1.5,1.5,3,6,12,18,35,50,65,80 % of the peak.

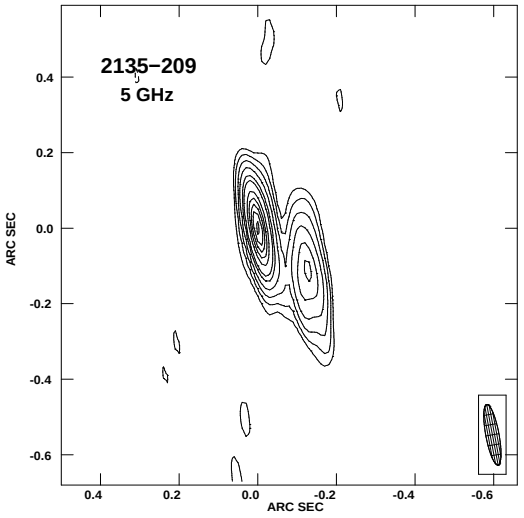

Fig. 9. PKS 2135-209 at 4993 MHz from the MERLIN array. The peak level is 1.02 Jy/beam and contours are shown at -0.75,0.75,1.5,3,6,12,18,35,50,65,80,95 % of the peak.

Dallacasa et al. (1995) have investigated a sample of northern CSS sources (using MERLIN and EVN) selected from the Peacock & Wall catalogue (1981). As their sample and the present sample have the same selection and observing frequencies, it is expected that sources in both samples should have, on average, similar characteristics. CSS sources selected from the Wall & Peacock sample tend to have a higher turnover frequency and smaller size (e.g. Dallacasa et al. 1995) because of the higher selection frequency (*i.e.* 2.7GHz) compared with the 3CR sample (178 MHz).

The size of the sources in the present sample range between ∼0.08 and ∼2.9 kpc, similar to the range found in the sample studied in Dallacasa *et al.* (1995), and smaller than the 3CR samples (Fanti *et al.* 1990 and references therein). Turnover frequencies are in the range around 0.1 – 0.2 GHz or below, with the exception of 1934-63 that peaks at ∼ 1.4GHz. As expected from the correlation between the linear size of the source and the turnover frequency (Fanti et al. 1990), the smallest source in our sample is the GPS source $1934-638$, that has the turnover at higher frequency.

Dallacasa et al. (1995) also find that most of galaxies their PW CSS sample show weak core candidates at $\lesssim 2\%$ of the total flux density, in contrast with the 3CR samples, where, however, the dynamic range was smaller and comparable to these achieved for most of the sources presented in this paper.

Of the seven CSS/GPS objects presented in this paper, four have been searched for HI absorption (0023-26, 1814-63, 1934-63 and 2135-20). The results have been summarised in Morganti et al. (2001) while the preliminary results from new VLBI observations for 1814-63 have been presented in Morganti et al.(2000).

Of the four objects, three are detected. The only one undetected is 2135-209, but this result is not too surprising given that it is classified as broad-line galaxy. It is interesting, however, that the most impressive HI absorption is detected in the object with the most complex radio structure in our small sample, 1814-63. The deep HI absorption appears extended and cover most of the source with the exception of the southern part of the southern lobe. The peak optical depth goes from ∼ 30% in the southern lobe to ∼ 10% in the northern region. The component with lower optical depth (ranging between 2 and 4%) is observed *only* against the northern region. Using the available systemic velocity ($V_{\rm hel}$ = 19350 km s^{-1}, Morganti et al. 2001), most of the H I absorption appears to be blueshifted. This can be explained by the presence of extended gas, possibly surrounding the lobes, interacting/expanding with the radio plasma. Therefore, in the case of 1814-63, part of the radio morphology could be affected by a strong interaction with the ISM.

Overall, the properties of the sources discussed here are consistent with the results from the analysis of other samples of CSS sources. In a forthcoming paper we will discuss their properties in wavebands different from radio, compare them with those of extended radio sources and verify whether they support and *"youth"* scenario.

References

Axon D.J., Capetti A., Fanti R. et al. 2000, AJ 120, 2284

Bicknell J., Dopita M., O'Dea C. 1997, ApJ 485, 112

Clark, B.G., 1973, Proc. IEEE, 61, 1242

Conway J.E. 1996, in " The second Workshop on Gigahertz Peaked Spectrum and Compact Steep Spectrum Radio Sources", Eds. Snellen, Schilizzi et al. M.N. Publ JIVE, Leiden p.198

Dallacasa D., Fanti C., Schilizzi R.T., Spencer R.E., 1995, A&A 295, 27

Fanti C., Pozzi F. Fanti R. et al. 2000, A&A 358, 499

Fanti R., Fanti C., Schilizzi R.T. et al. 1990, A&A 231, 333

Fanti, C., Fanti, R., Dallacasa D. et al. 1995 A&A 302, 317

Fanti C., 2000, "Proceedings of the 5th European VLBI Network Symposium" J.E. Conway, A.G. Polatidis, R.S. Booth and Y.M. Pihlström ISBN 91-631-0548-9, p. 73

Gelderman R. & Whittle M. 1994, ApJS 91,491

Jauncey D.L., Wright A.E., Peterson B.A. & Condon J. 1978, ApJ 219, L1

Jauncey D.L. & the SHEVE Team 1994, in "Very high angular resolution imaging", IAU158, J. G. Robertson and William J. Tango., eds., Dordrecht: Kluwer, p. 131

Kellerman K.I. 1966 ApJ 146, 621

King E. 1994 PhD Thesis Univ. of Tasmania

Morganti, R., Killeen, N.E.B. & Tadhunter, C.N. 1993, MNRAS, 263, 1023

Morganti R., Oosterloo T., Tadhunter C.N., van Moorsel, Killeen N. & Wills K.A. 2001, MNRAS 323, 331

Morganti R., Oosterloo T.A., Reynolds J., Tadhunter C.N. & Migenes V. 1997, MNRAS, 284, 541

Morganti R., Oosterloo T.A., Tadhunter C.N. et al. 1999, A&A Suppl. 140, 355

Morganti R., Oosterloo T., Tadhunter C.N. et al. 2000, 'Proceedings of the 5th European VLBI Network Symposium' J.E. Conway, A.G. Polatidis, R.S. Booth and Y.M. Pihlström ISBN 91-631-0548-9, p. 111 (astro-ph/0010482)

Murgia M. et al. 1999 A&A 345, 769

O'Dea, C.P., Baum, S.A. & Stanghellini, C., 1991, ApJ 380, 66

O'Dea, C.P. 1998 PASP 110, 493

O'Dea C.P., de Vries W.H., Koekemoer A.M. et al. 2002 AJ accepted

Owsianik I. & Conway J.E.1998, A&A 337, 69

Padovani P., Morganti R., Siebert J., Cimatti A. & Vagnetti F. 1999, MNRAS, 304, 829

Peck A.B., Taylor G.B. 2001, ApJ 554, L147

Penston M.V. & Fosbury R.A.E. 1978, MNRAS 183, 479

Pihlström Y.M. 2001, PhD. Thesis, Chalmers University & Onsala Observatory

Preston & the SHEVE Team, 1993, in *Sub-arcsecond Radio Astronomy*, eds. R.J. Davis and R. S. Booth, Cambridge University Press, 1993., p.428

di Serego Alighieri S., Danziger J.I., Morganti R. & Tadhunter C., 1994, MNRAS 269, 998

de Vries W., O'Dea C.P., Baum S.A. et al. 1998, ApJ 503, 138

Sanghera H.S. 1993, PhD Thesis, Univ. of Manchester

Shepherd, M. C., Pearson, T. J., & Taylor, G. B. 1994, BAAS, 26, 987

Siebert, J., Brinkmann W., Morganti, R. et al. 1996, MNRAS 279, 1331
Silk J., Rees M.J. 1998, A&A 331, L1
Spencer, R.E., Schilizzi, R.T., Fanti et al. 1991, MNRAS, 250, 225
Tadhunter, C.N., Morganti, R., di Serego Alighieri, S., Fosbury, R.A.E. & Danziger, I.J. 1993, MNRAS, 263, 999
Tadhunter C.N., Shaw M. & Morganti R. 1994. MNRAS, 271, 807
Tadhunter C.N., Morganti R., Robinson A. et al. 1998, MNRAS, 298, 1035
Trussoni E., Vagnetti F., Massaglia S. et al. 1999, A&A 348, 437
Tzioumis et al. 1996, in *The second Workshop on Gigahertz Peaked Spectrum and Compact Steep Spectrum Radio Sources*, Eds. Snellen, Schilizzi et al. M.N. Publ JIVE, Leiden p. 58
Venturi T., Morganti R., Tzioumis A. & Reynolds J., 2000 A&A 363, 84
Wall J. & Peacock J. 1985, MNRAS 216, 173

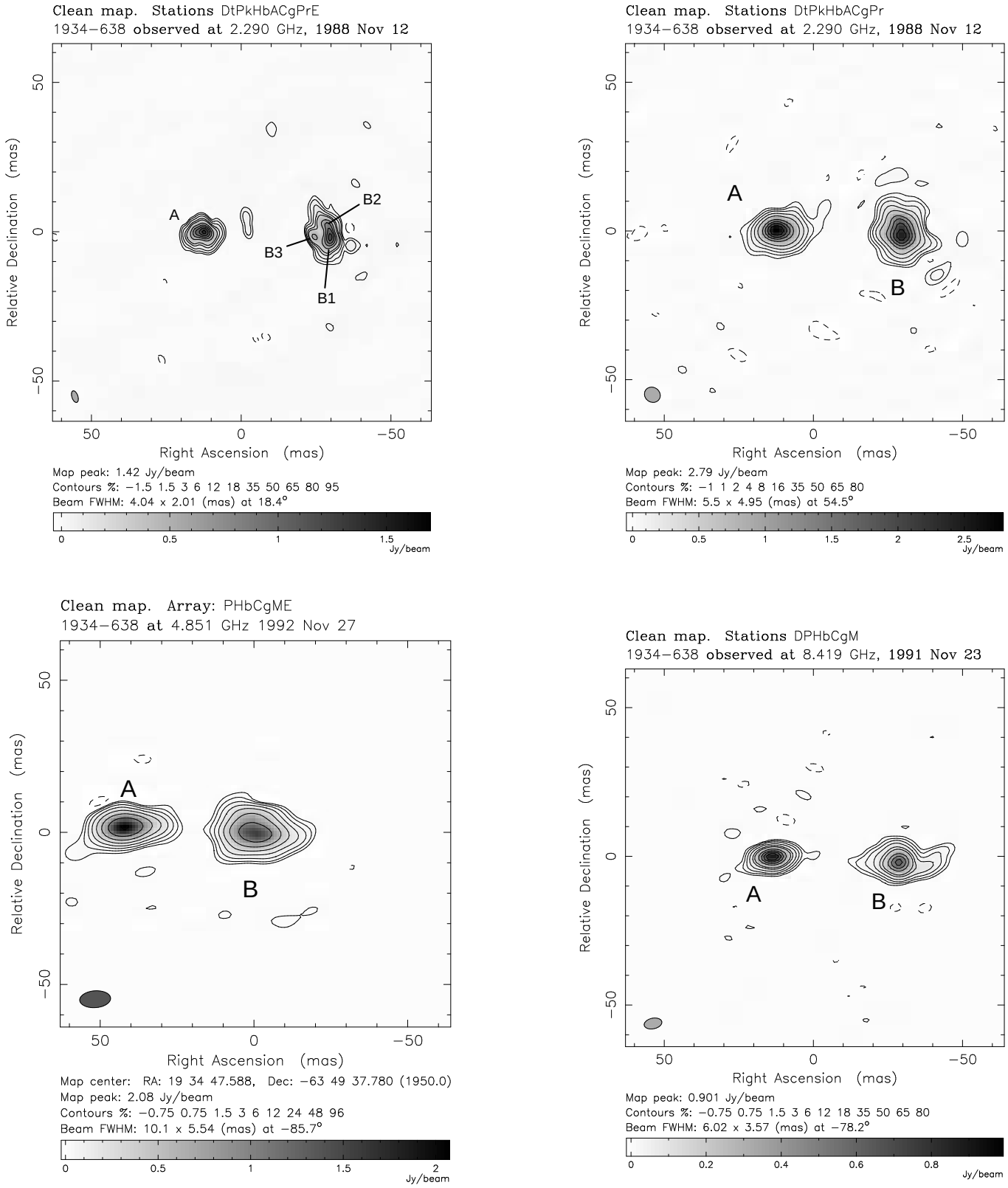

Fig. 10. VLBI images of PKS 1934-638 at 2.3, 4.8 and 8.4 GHz (from Tzioumis et al. 1997). The top-right image is at a higher resolution because it includes Hartebeesthoek data. The other three images have approximately the same resolution of about 5 mas.

This figure "fig4.jpg" is available in "jpg" format from:

http://arXiv.org/ps/astro-ph/0207495v1